Research Paper

MicroRNA therapy confers anti-senescent effects on doxorubicin-related cardiotoxicity by intracellular and paracrine signaling

Wenzheng Xia[1,2,*], Bowen Chang[3,*], Liqun Li[2], Tingting Hu[4], Jiaqi Ye[4], Hanbin Chen[4], Wenfeng Li[4], Tao Zan[1,*], Meng Hou[4,*,&]

[1]Department of Plastic and Reconstructive Surgery, Shanghai Ninth People's Hospital, Shanghai Jiao Tong University School of Medicine, Shanghai, Shanghai, China
[2]Department of Plastic Surgery, First Affiliated Hospital, Wenzhou Medical University, Wenzhou, Zhejiang, China
[3]Department of Neurosurgery, The First Affiliated Hospital of USTC, Division of Life Sciences and Medicine, University of Science and Technology of China, Hefei, Anhui, China
[4]Department of Radiation Oncology, First Affiliated Hospital, Wenzhou Medical University, Wenzhou, Zhejiang, China
*Equal contribution

Correspondence to: Tao Zan, Meng Hou; **email:** zantaodoctor@yahoo.com, https://orcid.org/0000-0002-4810-9668; 244517813@qq.com, https://orcid.org/0000-0002-6304-724X
Keywords: doxorubicin, cardiotoxicity, microRNA, senescence, exosome
Received: April 11, 2021 **Accepted:** November 22, 2021 **Published:** December 5, 2021

ABSTRACT

Doxorubicin (Dox), an important anthracycline, is a potent anticancer agent that is used for treating solid tumors and hematologic malignancies. However, its clinical use is hampered by cardiac cardiotoxicity. This study aimed to investigate the cardioprotective potential of miR-199a-3p. Continuous Dox treatment not only markedly induced cardiomyocyte senescence but also resulted in a growing number of senescence-associated secretory phenotype (SASP) cardiomyocytes, frequently leading to heart senescence. This study showed that miR-199a-3p was downregulated in cardiomyocytes when exposed to Dox. The cardiac-specific overexpression of miR-199a-3p promoted cell cycle re-entry and cell proliferation, resulting in relief from cardiac senescence. Also, the elevation of miR-199a-3p inhibited the generation of SASP, thus, hampering the spread of senescence. In cardiomyocytes, the modulation of miR-199a-3p changed the levels of senescence-related protein GATA4. The ectopic expression of GATA4 blunted the anti-senescence effect of miR-199a-3p. Together, the data supported a role for miR-199a-3p during Dox cardiotoxicity. The elevation of miR-199a-3p might provide a dual therapeutic advantage in Dox cardiotoxicity therapy by simultaneously preventing cardiac senescence and reducing the spread of senescence.

INTRODUCTION

Anthracyclines are among the most potent and widely prescribed chemotherapeutics since the last century and still are the cornerstones of cancer treatment in combination with new therapies [1]. However, the clinical use of these drugs, is restricted by cardiotoxicity, often suggesting modification or even discontinuation of potentially successful anticancer regimens [2]. Cardiotoxicity commonly happens within the first year after therapy completion, as lifespans are lengthened, thus elevating morbidity and mortality among cancer survivors [3].

Although clinical assessment allows the early detection of cardiotoxicity, validated prevention and treatment represent still-unmet clinical needs. Thus, an increasing number of oncologists have focused on optimal cardioprotective treatments and mechanisms [4]. A previous study suggested that Dox-related cardiotoxicity may result from cardiomyocyte senescence [5]. Demaria et al. has suggested that eliminating therapy-

induced senescent cells alleviated several short- and long-term effects of the drugs, including cardiac dysfunction, bone marrow suppression, even cancer recurrence [6]. Persistent cellular senescence caused chromatin reorganization and acquisition of a secretome composed of cytokines, chemokines, and extracellular matrix factors, all known as the senescence-associated secretory phenotype (SASP) [7, 8]. Previous studies showed that senescent cardiomyocytes acquired an SASP that negatively affected healthy nonsenescent cardiomyocytes, rendering them senescent [9]. Ideally, optimal cardioprotective treatments should not only interfere with alleviating cardiomyocyte senescence but also reduce the spread of senescence.

MicroRNAs exhibited regulating entire gene expression networks and taking significant effect in cardiovascular diseases [10]. Although several studies have examined the regulation of cardiac senescence by microRNAs [11, 12], less is known about their functional roles in this context. Previously, functional screening identified many miRNAs that had the potential to exert an anti-senescent effect and induce cardiac regeneration [13]. Among these, miR-199a-3p, upon intra-cardiac injection, was shown to stimulate cardiomyocyte proliferation and promote cardiac regeneration [14, 15]. This study explored the therapeutic potential of miR-199a-3p in cardiac regeneration and protection against Dox-related cardiotoxicity.

GATA4 is one of the outstanding factors regulating both developmentally programmed senescence and damage-induced senescence [16]. GATA4, which is evolutionarily conserved, participates in an extensive range of biological processes, including cell cycle control, DNA damage, and energy metabolism, thus, contributing to tissue senescence [17, 18]. GATA4 serves as a prominent switch in the senescence regulatory network to activate SASP [16]. *In vivo* and *in vitro* models confirmed that GATA4 activated by SASP or other developmental cues regulated senescence via the upregulation of p16 in damage-induced and developmental senescence, which was an important factor in Dox-related cardiotoxicity [19]. These findings indicated that GATA4 took significant effect in senescence as one of the prominent sensors mediating senescent signaling in response to environmental stresses. Therefore, modulating this factor might alleviate Dox-related cardiotoxicity.

This study identified miR-199a-3p as a prominent determinant of anthracycline cardiotoxicity and provided a proof of concept that modulating miR-199a-3p/GATA4 was an incomparable means of preventing Dox cardiotoxicity, while inhibiting the spread of senescence. The genetic induction of miR-199a-3p elevation might provide a new approach against anthracycline-induced heart disease.

RESULTS

Dox-treated cardiomyocytes exhibited increased cellular senescence

The flow cytometry analysis of the cellular cycle revealed an increased number of cardiomyocytes trapped in the G0/G1 phase in the Dox-treated group (Figure 1A, 1B). The cell growth curves showed that Dox-treated cardiomyocytes exhibited lower proliferative ability compared to control cells (Figure 1C). Furthermore, the cells in the Dox-treated group exhibited increased levels of senescence-associated β-galactosidase (SA-β-gal) activity (Figure 1D, 1E). Additionally, $p16^{INK4a}$ immunostaining showed that cellular senescence was activated in the Dox-treated cardiomyocytes (Figure 1F). Taken together, these data showed that Dox-treated cardiomyocytes exhibited increased cellular senescence. Interestingly, the decreased level of miR-199a-3p was found in Dox-treated cardiomyocytes and mouse heart tissue, which was confirmed by qRT-PCR (Figure 1G, 1H). At meanwhile, more $p16^{INK4a}$ -positive cells presented in the Dox -treated animals compared with the controls (Figure 1I).

A slowdown of Dox-induced aging via the overexpression of miR-199a-3p

The study simultaneously investigated whether inducing miR-199a-3p could slow down the progression of aging. To do so, miR-199a-3p mimic transfection was performed to induce miR-199a-3p overexpression (Figure 2A). Hence, the study examined whether the elevation of miR-199a-3p in these Dox-treated cells might help overcome cellular senescence. Compared to the control cells, Dox-treated cardiomyocytes were distributed more in the G0/G1 phase, with impaired proliferative ability, while miR-199a-3p-overexpressing cardiomyocytes demonstrated a recovery in the cellular cycle and proliferation (Figure 2B, 2C). Then, SA-β-gal staining and SASP test were used to study aging-related physiology. Compared to the Dox-treated groups, the Dox+ miR-199a-3p mimic group displayed accelerated declines in SA-β-gal-positive cells and SASP (Figure 2D–2F). Telomere length and telomerase activity tests revealed that Dox-treatment caused a decline more than that in the control, while the elevation of miR-199a-3p slowed the speed of aging (Figure 2G, 2H). At meanwhile, latter after Dox treatment, cellular viability impaired and apoptosis happened, miR-199a-3p overexpression showed protective effect against apoptosis (Supplementary Figure 1A–1C).

MiR-199a-3p directly targeted GATA4

TargetScan was used to predict the targets of miR-199a-3p. Among the predicted genes, GATA4 was chosen for further analysis, which was reported to participate in the heart senescence process [16]. To assess whether GATA4 was a direct target of miR-199a-3p, a 3'-UTR GATA4 reporter construct was used to assess the direct

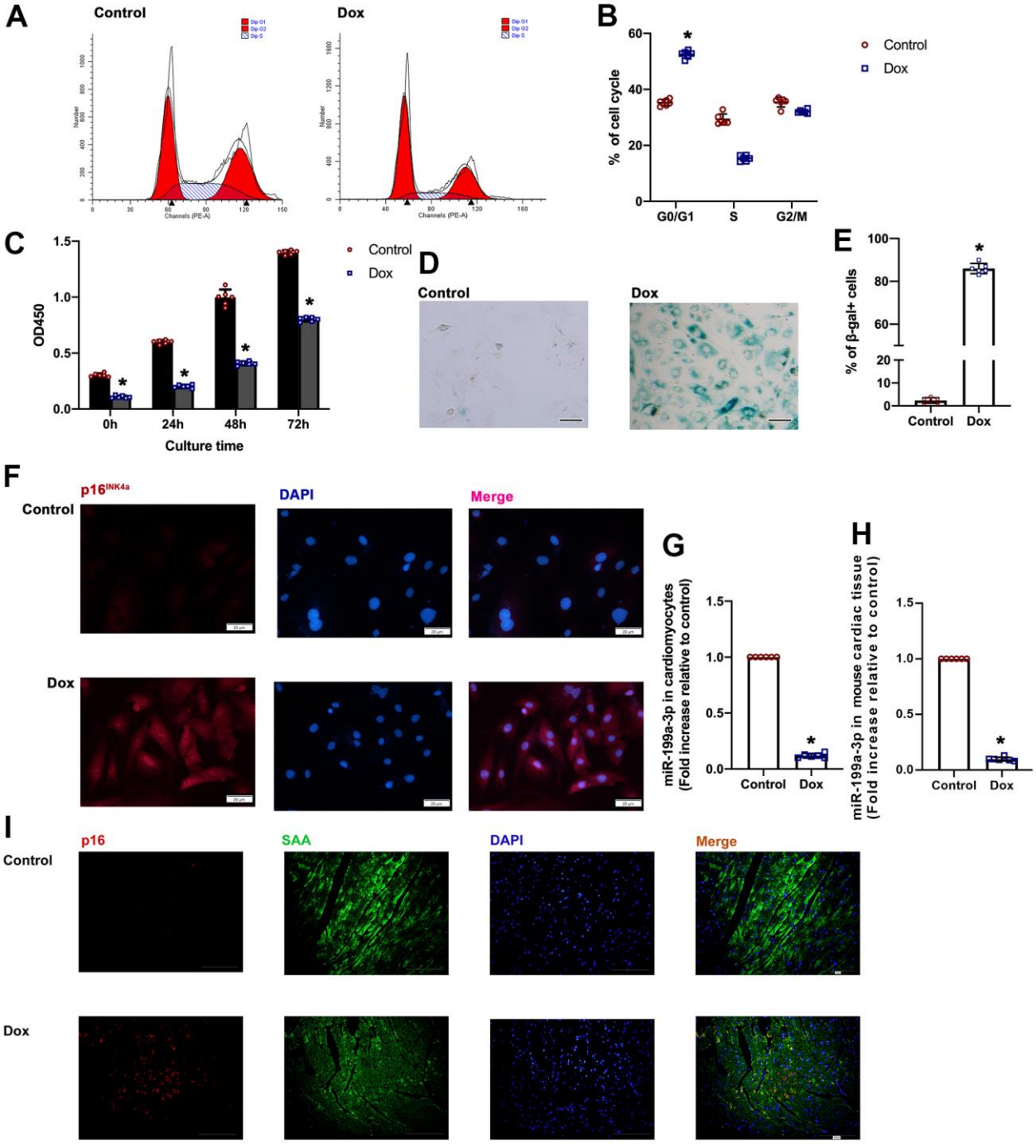

Figure 1. Dox-treated cardiomyocytes exhibited increased cellular senescence. (**A**) Cell cycle analysis was performed with PI staining by flow cytometry. (**B**) Percentages of cells in the three phases of the cell cycle. (**C**) Cellular proliferation was measured using CCK-8 assay. (**D**) Representative images of SA-β-gal staining (senescent cells are stained green). Scale bars, 20 μm. (**E**) Percentage of senescent cells was calculated. (**F**) Representative $p16^{INK4a}$ staining (green). Scale bars, 20 μm. (**G**, **H**) Expression of miR-199a-3p in cardiomyocytes and cardiac tissue was quantified by qRT-PCR. $^{*}P < 0.05$ versus control, $n = 6$ per group. (**I**) Representative photomicrographs of $p16^{INK4a}$-positive cardiomyocytes in the Dox treated cardiac tissue. Scale bars, 100 μm.

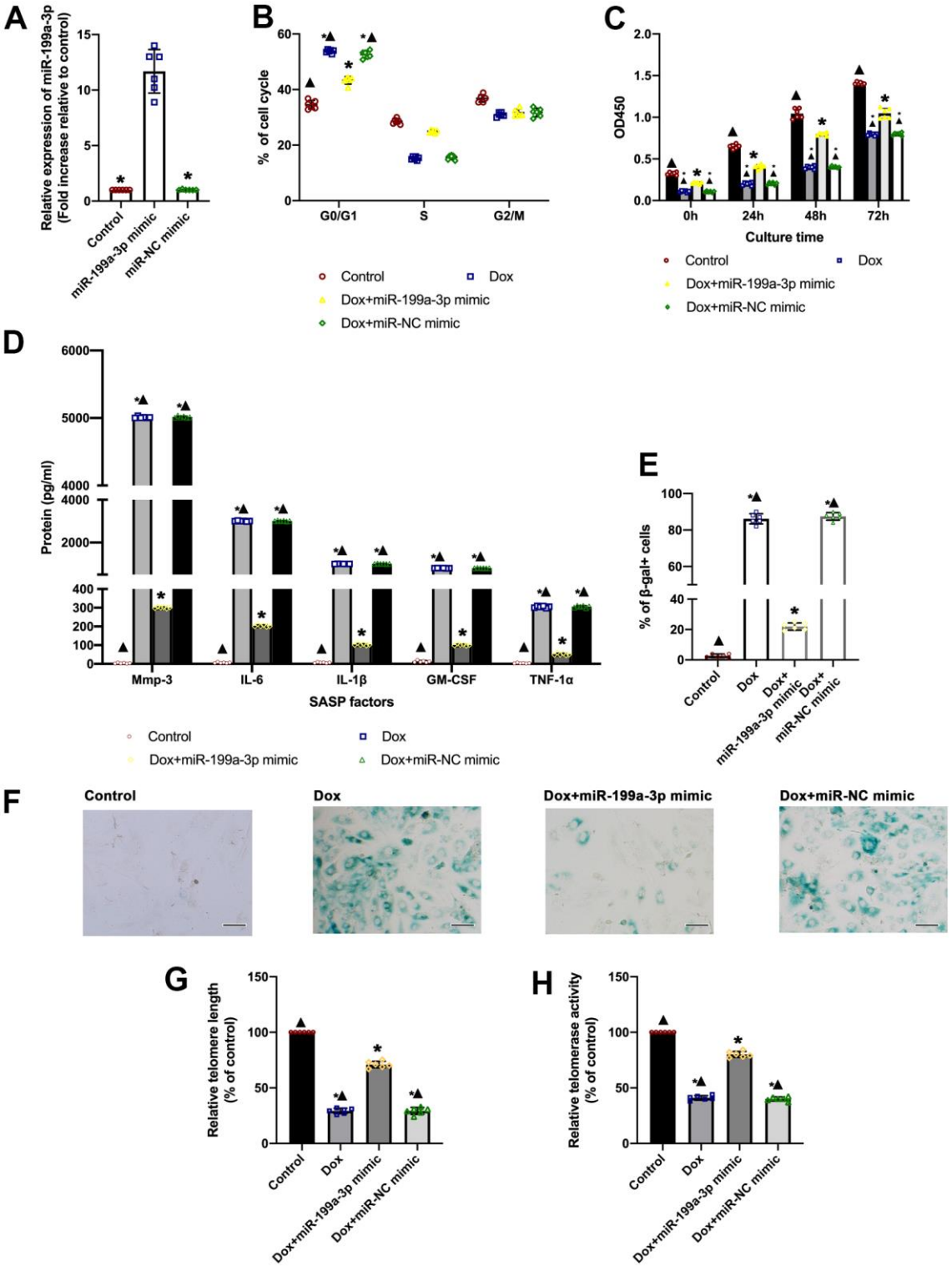

Figure 2. A slowdown of Dox-induced aging via the overexpression of miR-199a-3p. (**A**) Expression of miR-199a-3p was quantified by qRT-PCR. $^{*}P < 0.05$ versus the miR-199a-3p mimic in repeated-measures ANOVA, $n = 6$ per group. (**B**) Percentages of cells in the three phases of the cell cycle determined by flow cytometry. (**C**) Cellular proliferation was measured by the CCK-8 assay. (**D**) SASP factor protein levels quantified by Luminex of the medium. The medium was collected from such cells as follows: transfection with the miR-199a-3p mimic or miR-NC mimic, followed by treatment with Dox. The untreated cardiomyocytes were used as control. (**E**) The percentage of senescent cells was calculated. (**F**) Representative images of SA-β-gal staining (senescent cells are stained green). Scale bars, 20 μm. (**G**) Telomere length was detected by qRT-PCR. (**H**) Telomerase activity was determined using a telomerase repeat amplification protocol (TRAP). $^{*}P < 0.05$ versus control; $^{▲}P < 0.05$ versus Dox + miR-199a-3p mimic in repeated-measures ANOVA, $n = 6$ per group.

binding of miR-199a-3p to GATA4 mRNA. The overexpression of an miR-199a-3p mimic compared with control significantly decreased luciferase reporter activity, suggesting that miR-199a-3p bound directly to GATA4 mRNA (Figure 3A, 3B). The study also detected the protein of GATA4 in Dox, Dox + miR-199a-3p mimic, and Dox + miR-NC mimic groups. The GATA4 protein level was higher in the Dox group compared to the control, while it decreased in the Dox + miR-199a-3p mimic group (Figure 3C, 3D).

MiR-199a-3p repressed GATA4 contributing to the anti-senescent effect against Dox

Ad-GATA4 was designed to induce the overexpression of GATA4 so as to test whether the anti-senescent effect of this miRNA in Dox-treated cardiomyocytes could be due to the inhibition of GATA4 (Figure 4A–4C). Through co-infection with the miR-199a-3p mimic and Ad-GATA4, it was confirmed that this approach led to the reduced anti-senescent effect of miR-199a-3p against Dox. For comparison, cell cycle and cellular proliferation were analyzed. Dox trapped more cells in the G0/G1 phase and inhibited proliferation, while miR-199a-3p relieved this. This anti-senescent effect was reversed by the co-infection with miR-199a-3p mimic and Ad-GATA4 (Figure 4D, 4E). The maintenance of GATA4 levels in Dox-treated cardiomyocytes preserved SA-β-gal+ and SASP cardiomyocytes, which was decreased by miR-199a-3p mimic (Figure 4F–4H). Of note, GATA4 overexpression was effective in reducing telomere length and telomerase activity, which was recovered by miR-199a-3p mimic transfection against Dox (Figure 4H, 4I).

MiR-199a-3p eliminated the spread of senescence among cardiomyocytes

A subset of Dox-treated cardiomyocytes expressed SASP factors, and the SASP factors were inhibited by

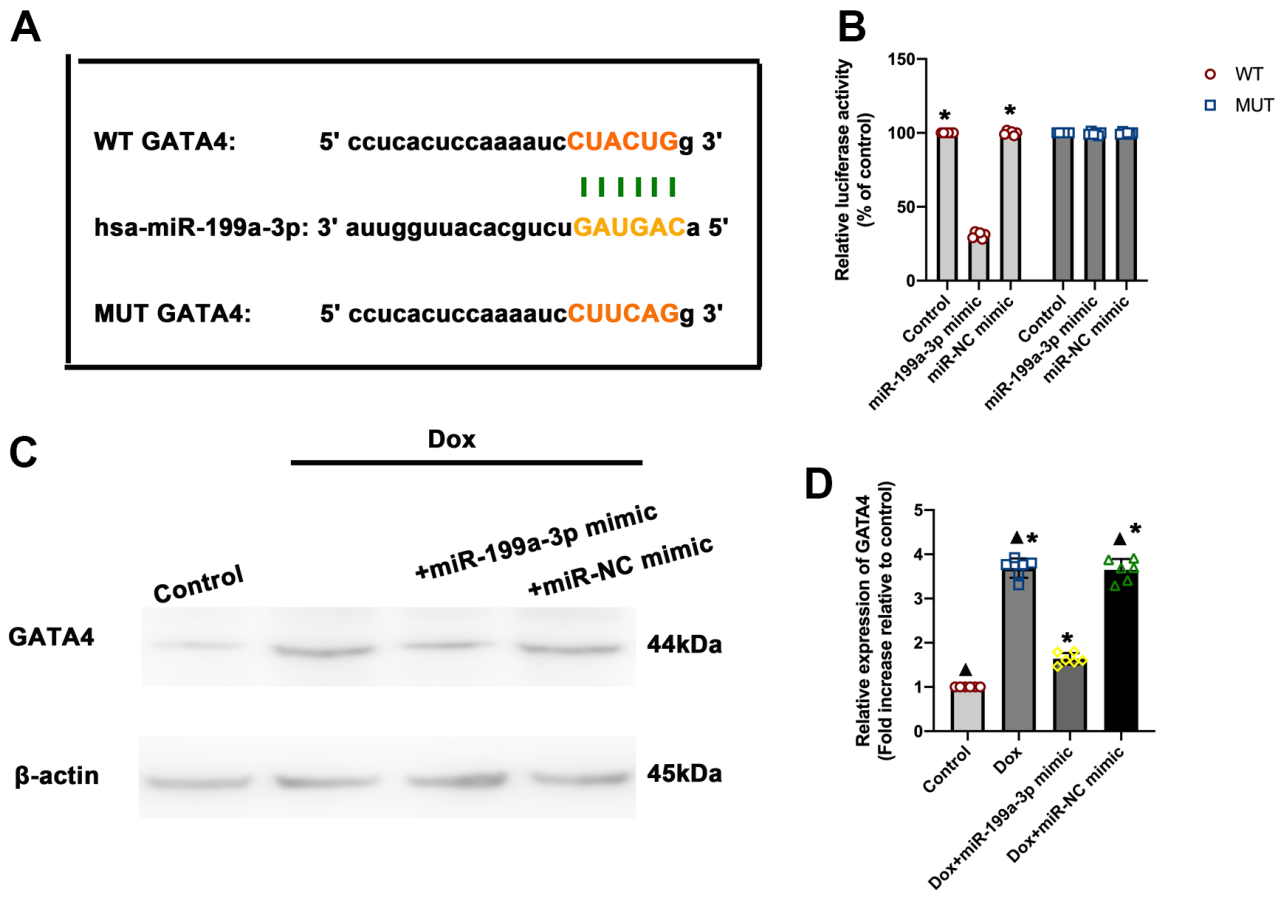

Figure 3. MiR-199a-3p directly targeted GATA4. (**A**) Predicted miR-199a-3p binding site in the 3'-UTR of GATA4. The corresponding sequence in the mutated (MUT) version is also shown. (**B**) Luciferase activity was analyzed 48 h after transfection of the miR-199a-3p mimic or miR-NC mimic. $^{*}P < 0.05$ versus the miR-199a-3p mimic (WT group) in repeated-measures ANOVA, $n = 6$ per group. (**C, D**) Western blot analysis of GATA4. The size of markers (in kDa) is indicated. $^{*}P < 0.05$ versus control; $^{▲}P < 0.05$ versus Dox + miR-199a-3p mimic in repeated-measures ANOVA, $n = 6$ per group.

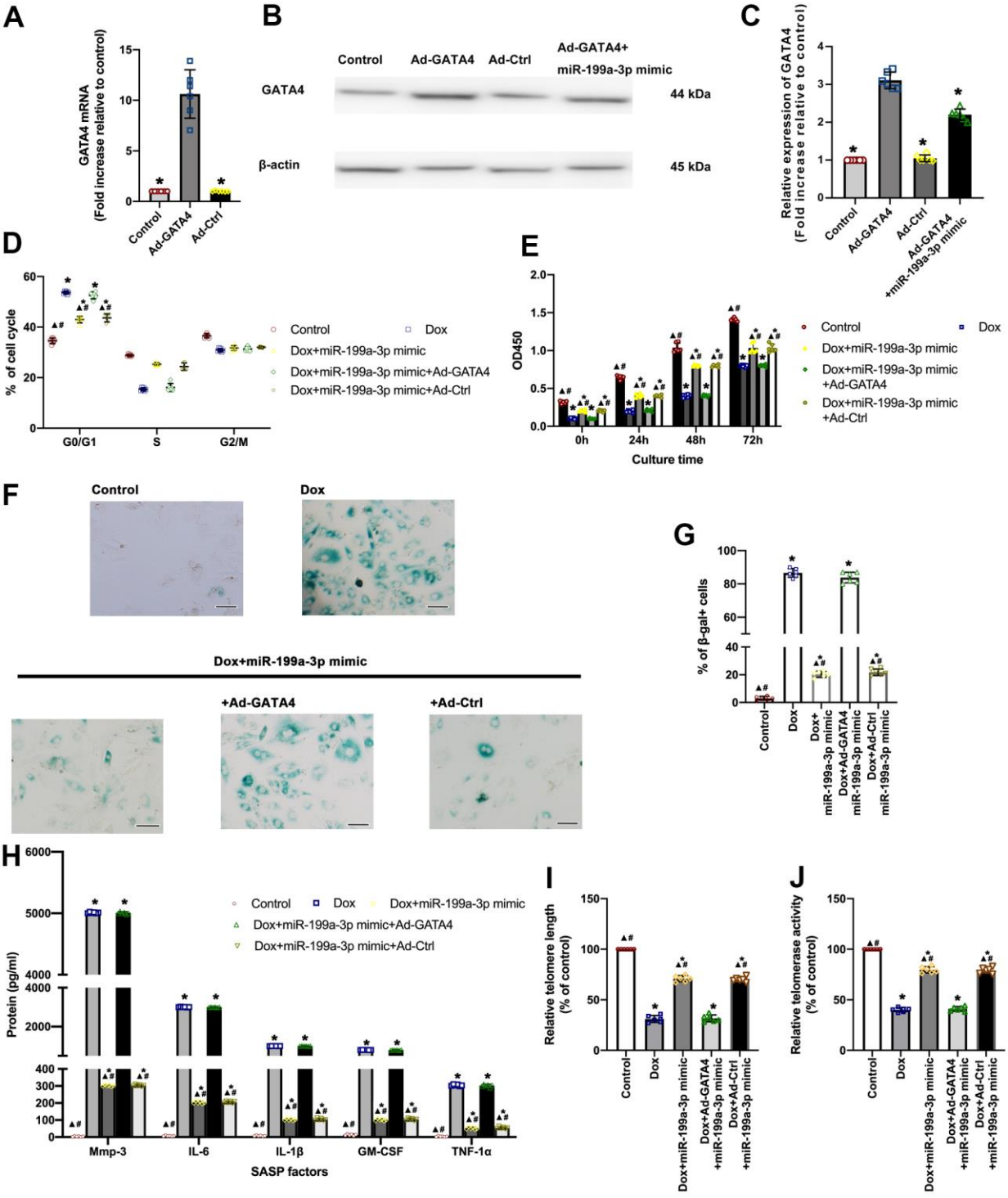

Figure 4. MiR-199a-3p repressed GATA4 contributing to the anti-senescent effect against Dox. (**A**–**C**) Cardiomyocytes were infected with Ad-GATA4, Ad-Ctrl, or Ad-GATA4+miR-199a-3p mimic. After 24 h, the cell lysates were harvested for qRT-PCR (**A**) and western blot analysis (**B, C**). $^{*}P < 0.05$ versus Ad-GATA4 in repeated-measures ANOVA, $n = 6$ per group. (**D**) The percentages of cells in the three phases of the cell cycle determined by flow cytometry. (**E**) Cellular proliferation was measured using the CCK-8 assay. (**F**) Representative images of SA-β-gal staining (senescent cells are stained green). Scale bars, 20 μm. (**G**) The percentage of senescent cells was calculated. (**H**) SASP factor protein levels quantified by Luminex of the medium. The medium was collected from such cells as follows: transfection with the miR-199a-3p mimic or the miR-199a-3p mimic + Ad-GATA4, or the miR-199a-3p mimic + Ad-Ctrl, followed by exposure to Dox. The untreated cardiomyocytes were used as the control. (**I**) Telomere length was detected by qRT-PCR. (**J**) Telomerase activity was determined using telomerase repeat amplification protocol (TRAP). $^{*}P < 0.05$ versus control; $^{▲}P < 0.05$ versus Dox; $^{\#}P < 0.05$ versus Dox + miR-199a-3p mimic + Ad-GATA4 in repeated-measures ANOVA, $n = 6$ per group.

miR-199a-3p overexpression. Therefore, the present study explored whether miR-199a-3p overexpression could inhibit the spread of senescence among cardiomyocytes. To this end, exosomes were collected from cardiomyocytes (Figure 5A–5C), DiI staining showed that exosomes were swallowed by cardiomyocytes (Figure 5D). Exosomes derived from Dox-treated cardiomyocytes (exosome^{Dox}) caused the development of senescence, accompanied by impaired proliferation (Figure 5E) and more SA-β-gal+ cells (Figure 5F, 5G). The extent of SASP secretion from exosome^{Dox}-treated cardiomyocytes varied (Figure 5H). Notably, exosomes derived from miR-199a-3p + Dox-treated cardiomyocytes (exosome$^{Dox+miR-199a-3p\ mimic}$) failed to induce the spread of senescence compared with exosome^{Dox} (Figure 5D–5H).

DISCUSSION

The present study revealed miR-199a-3p as an important player of anthracycline cardiotoxicity and proposed miR-199a-3p overexpression as an effective methods of preventing the cardiac adverse effects of Dox, besides inhibiting the spread of senescence.

Although major efforts in understanding the mechanism of anthracycline-induced cardiotoxicity, the molecular and cellular details are still not yet fully uncovered [20, 21]. Potential mechanisms include the generation of ROS, causing DNA damage and mitochondrial dysfunction, thus, leading to cardiac senescence [1, 22]. One common character of senescent cells is an essentially irreversible cell cycle arrest, with quiescence of cell proliferation [23]. The present study revealed that more cells were trapped in the G0/G1 phase, with impaired cellular proliferation, when subjected to Dox. Senescent cells secrete many factors, including pro-inflammatory cytokines, chemokines and MMPs, collectively termed the SASP [24]. SASP constitutes a hallmark of senescent cells and mediates patho-physiological effects [25]. For example, the SASP reinforces and spreads senescence; meanwhile, SASP factors mediate developmental senescence [26, 27]. The results supported the notion that Dox not only caused cellular senescence but mediated the spread of senescence. A previous study raised the hope that inhibiting the spread of senescence could provide significant benefits in cardiac tissue regeneration [9], suggesting that it might be used to treat Dox-related cardiotoxicity. The findings showed that the alleviation of Dox-induced cardiomyocyte senescence could inhibit SASP, thus triggering a negative feedback loop and eventually inhibiting the spread of senescence.

A full understanding of the mechanism of Dox-related cardiac senescence remains elusive; however, the present study highlighted the role of miR-199a-3p in this process. Although miR-199a-3p expression has been associated with various disorders [28, 29], its precise functional role in cardiac diseases is still controversial. Minae An et al. reported that miR-199a-3p promoted cardiomyocyte growth and electrical activity, which in turn promoted electrical recovery and cardiac regeneration [30]. Anna Baumgarten et al. revealed that miR-199 was downregulated in dilated cardiomyopathy, thus, contributing to the loss of cardiac mass during the dilatation of the heart in the senescence process [31]. Keiichi Koshizuka et al. suggested that the miR-199 family inhibited cancer cell migration and invasion [32]. Such function can be used to identify a potential treatment for Dox-related cardiotoxicity, which meets the standard of the optimizing cardiac protective treatments in terms of not only interfering with the primary mechanisms of cardiotoxicity but at least preserving or even enhancing the antitumor efficacy of chemotherapy. Using the gain-of-function genetic approach in Dox-injured cardiomyocytes, it was found that the miR-199a-3p promoted cardiomyocyte proliferation and de-repressed cell cycle, thus, facilitating the recovery from senescence. These results concluded that the upregulation of miR-199a-3p might serve as an important regulatory component of a molecular pathway that alleviated the Dox-induced senescence. Meanwhile, exosomes and their miR cargo have been reported to act during intercellular communication in the cellular senescence process [33, 34]; miRs are packaged into exosomes to modulate cellular senescence and organismal aging [35]. Interestingly, the results revealed that exosome derived from Dox- treated cardiomyocytes induced senescence communication, while the spread of senescence was alleviated by miR-199a-3p overexpression.

MiR-199a-3p, same as other microRNAs, engages a broad series of mRNA targets, including numerous survival factors and cell cycle regulatory proteins to take effects [36, 37]. Thus, the potential promotion of the regenerative response by the miR-199a-3p involves the actions of protein targets that participate in cellular senescence [14]. The current study design pointed to an anti-senescence contribution of the miR-199a-3p via modulating GATA4. GATA4, as a key regulator of SASP and senescence, accumulates during cellular senescence [38, 39]. The SASP is manipulated by enhancer remodeling and activation of transcription factor GATA4 [16]. During the senescence process, this accumulated GATA4 initiates a transcriptional circuit to activate SASP [18]. In agreement, the findings revealed that Dox induced GATA4 accumulation, with the activation of SASP cardiomyocytes. In the aged chondrocytes, the inhibition of GATA4 suppressed SASP factors, leading to the relief from senescence

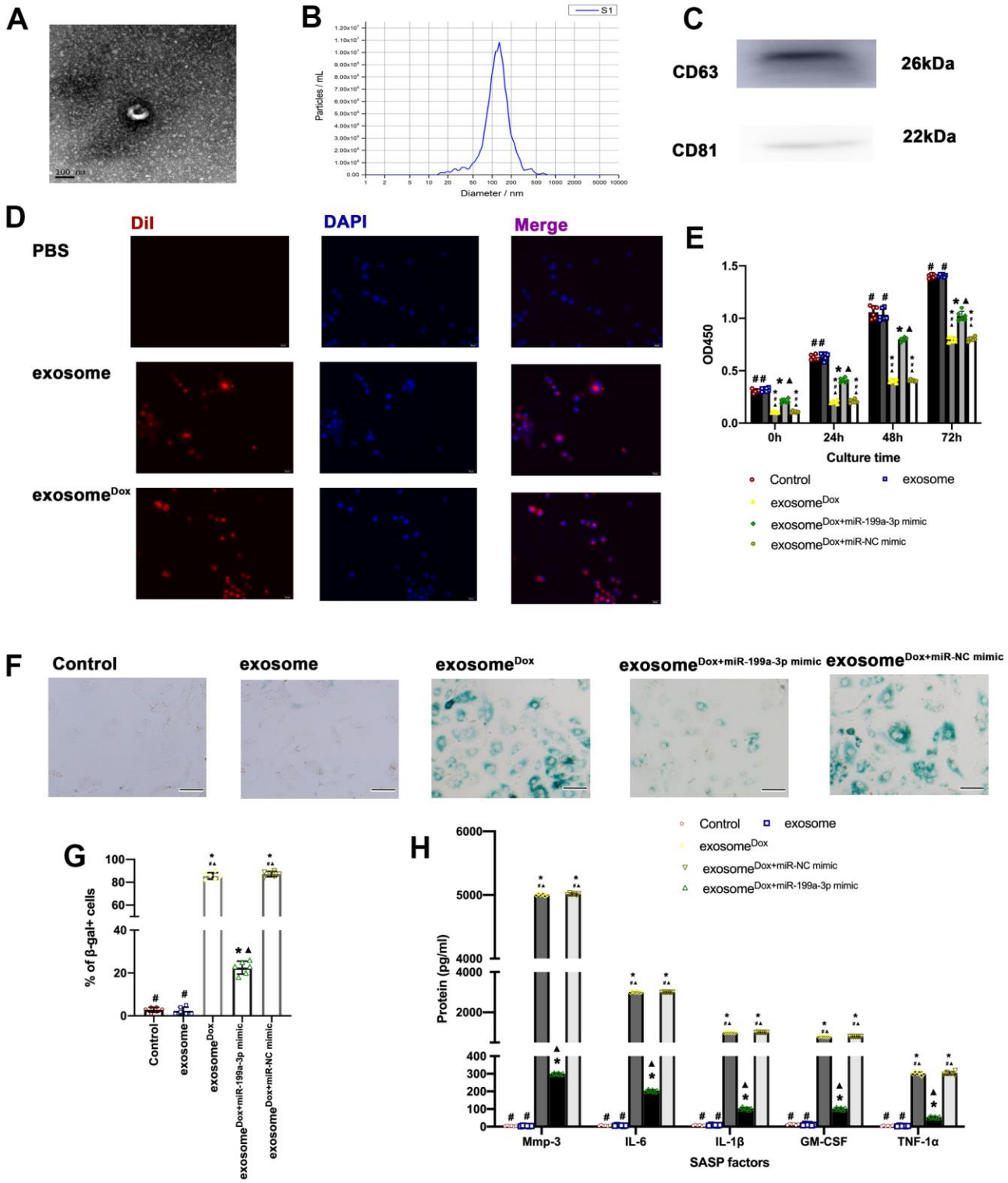

Figure 5. MiR-199a-3p eliminated the spread of senescence among cardiomyocytes. (**A**) Representative electron micrograph of isolated exosomes. Scale bar: 100 nm. (**B**) Size of exosomes measured using a Zetasizer Nano ZS instrument. (**C**) Protein levels of CD63 and CD81, two exosome markers. (**D**) DiI-labeled exosomes (red) were internalized into DAPI-labeled cardiomyocytes (blue). Scale bar, 20 μm. (**E**) Cellular proliferation was measured using the CCK-8 assay. (**F**) Representative images of SA-β-gal staining (senescent cells are stained green). Scale bars, 20 μm. (**G**) The percentage of senescent cells was calculated. (**H**) SASP factor protein levels quantified by Luminex of the medium. The medium was collected from cells as follows: treated with exosome, exosome^{Dox}, exosome$^{Dox+miR\text{-}199a\text{-}3p\ mimic}$, and exosome$^{Dox+miR\text{-}NC\ mimic}$. The untreated cardiomyocytes were used as control. $^{*}P < 0.05$ versus control; $^{▲}P < 0.05$ versus exosome; $^{\#}P < 0.05$ versus exosome$^{Dox+\ miR\text{-}199a\text{-}3p\ mimic}$ in repeated-measures ANOVA, $n = 6$ per group.

[40]. In similarities with this view, the findings of the present study showed that the prompt inhibition of GATA4 by miR-199a-3p ensured a general anti-senescence effect against Dox-related toxic effects.

Some limitations existed in the current study. The hiPSC-derived cardiomyocytes were applied to investigate the role of senescence in Dox cardiotoxicity, this may not comprehensive enough. Further investigation is required to explore the key experiments replicated in primary cardiomyocytes, which are post-mitotic and non-replicating cells.

CONCLUSIONS

Overall, miR-199a-3p might improve the prognosis of patients with cancer treated with Dox by concomitantly alleviating cardiomyocyte senescence as well as preventing the spread of senescence. Therefore, miR-199a-3p might eventually help "kill two birds with one stone" in patients with cancer requiring anthracycline chemotherapy.

MATERIALS AND METHODS

Animals

Male C57/Bl6 mice were maintained in accordance with the guidelines published by the US National Institutes of Health. During the experiments, mice were anesthetized with 1.5–2% isoflurane and kept warm on a heated platform. After the experiments, mice were sacrificed by CO_2 inhalation.

Cell culture and treatment

Human-induced pluripotent stem cell–derived cardiomyocytes

Human-induced pluripotent stem cell–derived cardiomyocytes were purchased from Cellular Dynamics International (WI, USA). The cells were cultured as previously described [5].

Dox treatment

The cardiomyocytes were cultured with Dox to model cardiac injury. The concentration of Dox was set at 0.5 μM and the exposure time at 24 h, as described previously [5].

Cell cycle assay

Further, 70% cold anhydrous ethanol was used to fix the cells. Then, the cells were treated with propidium iodide (PI) (Sigma, MO, USA) and RNase A. A flow cytometer equipped with Cell Quest software was used to detect cell cycle distribution, as described previously [41].

Cell proliferation assay

The cell counting kit-8 (CCK-8) assay was applied to estimate the cellular proliferation rate following the manufacturer's protocol. Briefly, the CCK-8 solutions were added in the cells grown in a 96-well plate, following incubated with for 1 h at 37° C, following which the absorbance of each well at 450 nm was recorded.

Senescence-associated β-galactosidase staining (SA-β-gal staining)

SA-β-gal staining was performed using a kit (Cell Signaling Technology, MA, USA) following the manufacturer's protocols. Senescent cardiomyocytes were identified as green-stained cells under light microscopy. Total cells were counted in three random fields per culture dish to determine the percentage of SA-β-gal-positive cells [42].

Immunofluorescence staining

Fixed with 4% PFA, the cardiomyocytes were treated with Triton X-100 at room temperature, blocked with 3% goat serum at 37° C, lasting for 1 h, and incubated with a primary antibody against $p16^{INK4a}$ (ab108349, 1:50) at 4° C overnight. The cells were subsequently incubated with secondary antibodies conjugated with Alexa Fluor 594, followed by DAPI staining. The images were captured using a Leica fluorescence microscope. The calculations were conducted in a blinded manner.

Immunofluorescent staining was performed with paraffin-embedded tissues. Primary antibodies used in this study included those against Cdkn2a ($p16^{Ink4a}$) (Abcam, ab211542), and Sarcomeric-α-actin (SAA; Invitrogen, 53-9760-82). Following primary incubation, slides were washed with 1X PBS and incubated with Alexa Fluor 594 (1:50; Invitrogen, A32740) secondary for one hour at room temperature. Sections were counterstained with DAPI staining medium and analyzed. Fluorescence was detected under a microscope.

Quantitative reverse transcription–polymerase chain reaction

Total RNA was extracted with TRIzol reagent (Invitrogen, CA, USA) and then subjected to a reverse transcription reaction using a First-Strand cDNA Synthesis kit (Roche). cDNA was used for real-time quantitative polymerase chain reaction (Q-PCR) analysis. Data were normalized by the level of U6, or GAPDH expression, in each sample.

Transfection with miR-199a-3p mimic

The miRNA mimic of miR-199a-3p was purchased from Invitrogen. The mirVana miRNA mimic was used to induce miR-199a-3p overexpression. Cardiomyocytes were transfected with a final concentration of 10 nmol/L for the miR-199a-3p mimic using an X-treme transfection reagent (Roche Applied Science, Penzberg, Germany) following the manufacturer's protocol.

Luminex assay

The levels of cytokines, chemokines, growth factors, and matrix metalloproteinases (MMPs) were measured in multiplex assays with the Luminex bead-based platform and software. Luminex assays were performed on 50 μL of cellular medium, according to the product instructions, as previously described [43]. After the cellular medium was collected, viable cell counts were determined from each sample to normalize data.

Relative telomere length measurement

Relative telomere length measurement in cardiomyocytes was performed using the PCR approach based on a previously established method [44], using Gapdh as the normalizing gene.

Relative telomerase activity measurement

The telomerase activity of cardiomyocytes was examined using a Telo TAGGG Telomerase PCR ELISA Plus kit following the manufacturer's protocols, as described previously [45].

Luciferase assay

Luciferase assays were conducted via cotransfection with a 3' -UTR-luciferase reporter plasmid and miRNA mimics (10nM) using Lipofectamine 2000 (Invitrogen). Luciferase activity was tested 48 h after transfection with a dual-luciferase reporter assay system (Promega, WI, USA) following the manufacturer's protocol.

Western blot analysis

Western blot analysis was conducted as previously described [46]. Primary antibodies, including GATA4 (ab256782, 1:1000), CD63 (ab59479, 1:750), and β-actin (ab179467) were purchased from Abcam. CD81 (#56039, 1:500) was purchased from Cell Signaling Technology.

Transient transfection

To overexpress of GATA4, the cardiomyocytes were transduced with adenoviral GATA4 (Ad-GATA4) or adenoviral control (Ad-Ctrl), as described previously [47]. The qRT-PCR and western blot analysis were conducted to confirm the transfection efficiency.

Isolation and tracing of exosomes

The exosomes were isolated and purified from the supernatants of cardiomyocytes. After 48 h of culture, the supernatants were collected. The exosome quick extraction solution was added to the filtered solution at a 1:5 ratio and stored at 4° C for at least 12 h. The characterization of exosomes was carried out as previously reported [46].

With respect to exosome tracing, the exosomes were labeled with DiI, followed by exosome isolation. With respect with the *in vitro* tracing of exosomes, DiI-labeled exosomes were incubated with the un-treated cardiomyocytes for 3 h. The cell nuclei were stained with DAPI, at a concentration of 1:1000 for 10 min at 37° C, as previously described [48]. The fluorescence was detected under a microscope.

Statistical analysis

Data were expressed as the mean ± standard deviation. Statistical significance of differences between groups was tested by repeated-measures analysis of variance (ANOVA). The Student's *t* test was used to compare the two groups. A *P*-value <0.05 indicated a statistically significant difference.

Abbreviations

Dox: Doxorubicin; SASP: senescence-associated secretory phenotype; miR: microRNA; qRT-PCR: quantitative reverse transcription–polymerase chain reaction; SA-β-gal assay: senescence-associated β-galactosidase assay; 3'-UTRs: 3′-untranslated regions; ROS: reactive oxygen species; DMEM: Dulbecco's modified Eagle's medium; PI: propidium iodide; CCK-8: cell counting kit-8; MMPs: matrix metalloproteinases; DAPI: 4′,6-Diamidine-2′-phenylindole dihydrochloride; DiI: 1,1'-dioctadecyl-3,3,3',3'-tetramethylindocarbocyanine perchlorate; SD: standard deviation; ANOVA: repeated-measures analysis of variance.

AUTHOR CONTRIBUTIONS

Wenzheng Xia: Provision of study material; Collection and/or assembly of data; Data analysis and interpretation; Bowen Chang: Conception and design; revising the article critically for important intellectual content; acquisition, analysis and interpretation of data; Liqun Li: Conception and design; Collection and/or assembly of

data; Data analysis and interpretation; Tingting Hu: Data analysis and interpretation; Manuscript writing; Jiaqi Ye: Collection and/or assembly of data; Data analysis and interpretation; Hanbin Chen: Collection and/or assembly of data; Data analysis and interpretation; Wenfeng Li: Conception and design; Financial support; Administrative support; Tao Zan: Revising the article critically for important intellectual content; drafting the article; Meng Hou: Conception and design; Manuscript writing; Final approval of manuscript.

CONFLICTS OF INTEREST

The authors declare that they have no conflicts of interest.

FUNDING

The present study was supported by the National Natural Science Foundation of China (Grant Nos. 82071561 to MH); the Youth Innovative Talents Support Program of Zhejiang Province Health Department (Grant No. 2022RC204 to MH); the Science and Technology Planning Project of Wenzhou (Grant No. Y2020735 to MH).

Editorial note

&This corresponding author has a verified history of publications using a personal email address for correspondence.

REFERENCES

1. Li M, Sala V, De Santis MC, Cimino J, Cappello P, Pianca N, Di Bona A, Margaria JP, Martini M, Lazzarini E, Pirozzi F, Rossi L, Franco I, et al. Phosphoinositide 3-Kinase Gamma Inhibition Protects From Anthracycline Cardiotoxicity and Reduces Tumor Growth. Circulation. 2018; 138:696–711. https://doi.org/10.1161/CIRCULATIONAHA.117.030352 PMID:29348263

2. Zamorano JL, Lancellotti P, Rodriguez Muñoz D, Aboyans V, Asteggiano R, Galderisi M, Habib G, Lenihan DJ, Lip GY, Lyon AR, Lopez Fernandez T, Mohty D, Piepoli MF, et al, and ESC Scientific Document Group. 2016 ESC Position Paper on cancer treatments and cardiovascular toxicity developed under the auspices of the ESC Committee for Practice Guidelines: The Task Force for cancer treatments and cardiovascular toxicity of the European Society of Cardiology (ESC). Eur Heart J. 2016; 37:2768–801. https://doi.org/10.1093/eurheartj/ehw211 PMID:27567406

3. Cardinale D, Colombo A, Bacchiani G, Tedeschi I, Meroni CA, Veglia F, Civelli M, Lamantia G, Colombo N, Curigliano G, Fiorentini C, Cipolla CM. Early detection of anthracycline cardiotoxicity and improvement with heart failure therapy. Circulation. 2015; 131:1981–88. https://doi.org/10.1161/CIRCULATIONAHA.114.013777 PMID:25948538

4. Lipshultz SE, Scully RE, Lipsitz SR, Sallan SE, Silverman LB, Miller TL, Barry EV, Asselin BL, Athale U, Clavell LA, Larsen E, Moghrabi A, Samson Y, et al. Assessment of dexrazoxane as a cardioprotectant in doxorubicin-treated children with high-risk acute lymphoblastic leukaemia: long-term follow-up of a prospective, randomised, multicentre trial. Lancet Oncol. 2010; 11:950–61. https://doi.org/10.1016/S1470-2045(10)70204-7 PMID:20850381

5. Xia W, Chen H, Xie C, Hou M. Long-noncoding RNA MALAT1 sponges microRNA-92a-3p to inhibit doxorubicin-induced cardiac senescence by targeting ATG4a. Aging (Albany NY). 2020; 12:8241–60. https://doi.org/10.18632/aging.103136 PMID:32384281

6. Demaria M, O'Leary MN, Chang J, Shao L, Liu S, Alimirah F, Koenig K, Le C, Mitin N, Deal AM, Alston S, Academia EC, Kilmarx S, et al. Cellular Senescence Promotes Adverse Effects of Chemotherapy and Cancer Relapse. Cancer Discov. 2017; 7:165–76. https://doi.org/10.1158/2159-8290.CD-16-0241 PMID:27979832

7. Childs BG, Durik M, Baker DJ, van Deursen JM. Cellular senescence in aging and age-related disease: from mechanisms to therapy. Nat Med. 2015; 21:1424–35. https://doi.org/10.1038/nm.4000 PMID:26646499

8. Kirkland JL, Tchkonia T. Cellular Senescence: A Translational Perspective. EBioMedicine. 2017; 21:21–28. https://doi.org/10.1016/j.ebiom.2017.04.013 PMID:28416161

9. Lewis-McDougall FC, Ruchaya PJ, Domenjo-Vila E, Shin Teoh T, Prata L, Cottle BJ, Clark JE, Punjabi PP, Awad W, Torella D, Tchkonia T, Kirkland JL, Ellison-Hughes GM. Aged-senescent cells contribute to impaired heart regeneration. Aging Cell. 2019; 18:e12931. https://doi.org/10.1111/acel.12931 PMID:30854802

10. Liu X, Xiao J, Zhu H, Wei X, Platt C, Damilano F, Xiao C, Bezzerides V, Boström P, Che L, Zhang C, Spiegelman BM, Rosenzweig A. miR-222 is necessary for exercise-induced cardiac growth and protects against pathological cardiac remodeling. Cell Metab. 2015; 21:584–95. https://doi.org/10.1016/j.cmet.2015.02.014 PMID:25863248

11. Boon RA, Iekushi K, Lechner S, Seeger T, Fischer A, Heydt S, Kaluza D, Tréguer K, Carmona G, Bonauer A, Horrevoets AJ, Didier N, Girmatsion Z, et al. MicroRNA-34a regulates cardiac ageing and function. Nature. 2013; 495:107–10. https://doi.org/10.1038/nature11919 PMID:23426265

12. Pulakat L, Chen HH. Pro-Senescence and Anti-Senescence Mechanisms of Cardiovascular Aging: Cardiac MicroRNA Regulation of Longevity Drug-Induced Autophagy. Front Pharmacol. 2020; 11:774. https://doi.org/10.3389/fphar.2020.00774 PMID:32528294

13. Eulalio A, Mano M, Dal Ferro M, Zentilin L, Sinagra G, Zacchigna S, Giacca M. Functional screening identifies miRNAs inducing cardiac regeneration. Nature. 2012; 492:376–81. https://doi.org/10.1038/nature11739 PMID:23222520

14. Gabisonia K, Prosdocimo G, Aquaro GD, Carlucci L, Zentilin L, Secco I, Ali H, Braga L, Gorgodze N, Bernini F, Burchielli S, Collesi C, Zandonà L, et al. MicroRNA therapy stimulates uncontrolled cardiac repair after myocardial infarction in pigs. Nature. 2019; 569:418–22. https://doi.org/10.1038/s41586-019-1191-6 PMID:31068698

15. Gao F, Kataoka M, Liu N, Liang T, Huang ZP, Gu F, Ding J, Liu J, Zhang F, Ma Q, Wang Y, Zhang M, Hu X, et al. Therapeutic role of miR-19a/19b in cardiac regeneration and protection from myocardial infarction. Nat Commun. 2019; 10:1802. https://doi.org/10.1038/s41467-019-09530-1 PMID:30996254

16. Kang C, Xu Q, Martin TD, Li MZ, Demaria M, Aron L, Lu T, Yankner BA, Campisi J, Elledge SJ. The DNA damage response induces inflammation and senescence by inhibiting autophagy of GATA4. Science. 2015; 349:aaa5612. https://doi.org/10.1126/science.aaa5612 PMID:26404840

17. Yamamura S, Izumiya Y, Araki S, Nakamura T, Kimura Y, Hanatani S, Yamada T, Ishida T, Yamamoto M, Onoue Y, Arima Y, Yamamoto E, Sunagawa Y, et al. Cardiomyocyte Sirt (Sirtuin) 7 Ameliorates Stress-Induced Cardiac Hypertrophy by Interacting With and Deacetylating GATA4. Hypertension. 2020; 75:98–108. https://doi.org/10.1161/HYPERTENSIONAHA.119.13357 PMID:31735083

18. Kang C, Elledge SJ. How autophagy both activates and inhibits cellular senescence. Autophagy. 2016; 12:898–99. https://doi.org/10.1080/15548627.2015.1121361 PMID:27129029

19. Chen L, Xia W, Hou M. Mesenchymal stem cells attenuate doxorubicin-induced cellular senescence through the VEGF/Notch/TGF-β signaling pathway in H9c2 cardiomyocytes. Int J Mol Med. 2018; 42:674–84. https://doi.org/10.3892/ijmm.2018.3635 PMID:29693137

20. Ichikawa Y, Ghanefar M, Bayeva M, Wu R, Khechaduri A, Naga Prasad SV, Mutharasan RK, Naik TJ, Ardehali H. Cardiotoxicity of doxorubicin is mediated through mitochondrial iron accumulation. J Clin Invest. 2014; 124:617–30. https://doi.org/10.1172/JCI72931 PMID:24382354

21. Zhang S, Liu X, Bawa-Khalfe T, Lu LS, Lyu YL, Liu LF, Yeh ET. Identification of the molecular basis of doxorubicin-induced cardiotoxicity. Nat Med. 2012; 18:1639–42. https://doi.org/10.1038/nm.2919 PMID:23104132

22. Liu D, Ma Z, Di S, Yang Y, Yang J, Xu L, Reiter RJ, Qiao S, Yuan J. AMPK/PGC1α activation by melatonin attenuates acute doxorubicin cardiotoxicity via alleviating mitochondrial oxidative damage and apoptosis. Free Radic Biol Med. 2018; 129:59–72. https://doi.org/10.1016/j.freeradbiomed.2018.08.032 PMID:30172748

23. He S, Sharpless NE. Senescence in Health and Disease. Cell. 2017; 169:1000–11. https://doi.org/10.1016/j.cell.2017.05.015 PMID:28575665

24. Coppé JP, Desprez PY, Krtolica A, Campisi J. The senescence-associated secretory phenotype: the dark side of tumor suppression. Annu Rev Pathol. 2010; 5:99–118. https://doi.org/10.1146/annurev-pathol-121808-102144 PMID:20078217

25. Nacarelli T, Lau L, Fukumoto T, Zundell J, Fatkhutdinov N, Wu S, Aird KM, Iwasaki O, Kossenkov AV, Schultz D, Noma KI, Baur JA, Schug Z, et al. NAD^+ metabolism governs the proinflammatory senescence-associated secretome. Nat Cell Biol. 2019; 21:397–407. https://doi.org/10.1038/s41556-019-0287-4 PMID:30778219

26. Acosta JC, Banito A, Wuestefeld T, Georgilis A, Janich P, Morton JP, Athineos D, Kang TW, Lasitschka F, Andrulis M, Pascual G, Morris KJ, Khan S, et al. A complex secretory program orchestrated by the inflammasome controls paracrine senescence. Nat Cell Biol. 2013; 15:978–90. https://doi.org/10.1038/ncb2784 PMID:23770676

27. Evangelou K, Lougiakis N, Rizou SV, Kotsinas A, Kletsas D, Muñoz-Espín D, Kastrinakis NG, Pouli N, Marakos P, Townsend P, Serrano M, Bartek J,

Gorgoulis VG. Robust, universal biomarker assay to detect senescent cells in biological specimens. Aging Cell. 2017; 16:192–97. https://doi.org/10.1111/acel.12545 PMID:28165661

28. Zhu G, Pei L, Lin F, Yin H, Li X, He W, Liu N, Gou X. Exosomes from human-bone-marrow-derived mesenchymal stem cells protect against renal ischemia/reperfusion injury via transferring miR-199a-3p. J Cell Physiol. 2019; 234:23736–49. https://doi.org/10.1002/jcp.28941 PMID:31180587

29. Li W, Wang L, Ji XB, Wang LH, Ge X, Liu WT, Chen L, Zheng Z, Shi ZM, Liu LZ, Lin MC, Chen JY, Jiang BH. MiR-199a Inhibits Tumor Growth and Attenuates Chemoresistance by Targeting K-RAS via AKT and ERK Signalings. Front Oncol. 2019; 9:1071. https://doi.org/10.3389/fonc.2019.01071 PMID:31681604

30. An M, Kwon K, Park J, Ryu DR, Shin JA, Lee Kang J, Choi JH, Park EM, Lee KE, Woo M, Kim M. Extracellular matrix-derived extracellular vesicles promote cardiomyocyte growth and electrical activity in engineered cardiac atria. Biomaterials. 2017; 146:49–59. https://doi.org/10.1016/j.biomaterials.2017.09.001 PMID:28898757

31. Baumgarten A, Bang C, Tschirner A, Engelmann A, Adams V, von Haehling S, Doehner W, Pregla R, Anker MS, Blecharz K, Meyer R, Hetzer R, Anker SD, et al. TWIST1 regulates the activity of ubiquitin proteasome system via the miR-199/214 cluster in human end-stage dilated cardiomyopathy. Int J Cardiol. 2013; 168:1447–52. https://doi.org/10.1016/j.ijcard.2012.12.094 PMID:23360823

32. Koshizuka K, Hanazawa T, Kikkawa N, Arai T, Okato A, Kurozumi A, Kato M, Katada K, Okamoto Y, Seki N. Regulation of ITGA3 by the anti-tumor miR-199 family inhibits cancer cell migration and invasion in head and neck cancer. Cancer Sci. 2017; 108:1681–92. https://doi.org/10.1111/cas.13298 PMID:28612520

33. Cortez MA, Bueso-Ramos C, Ferdin J, Lopez-Berestein G, Sood AK, Calin GA. MicroRNAs in body fluids--the mix of hormones and biomarkers. Nat Rev Clin Oncol. 2011; 8:467–77. https://doi.org/10.1038/nrclinonc.2011.76 PMID:21647195

34. Terlecki-Zaniewicz L, Lämmermann I, Latreille J, Bobbili MR, Pils V, Schosserer M, Weinmüllner R, Dellago H, Skalicky S, Pum D, Almaraz JC, Scheideler M, Morizot F, et al. Small extracellular vesicles and their miRNA cargo are anti-apoptotic members of the senescence-associated secretory phenotype. Aging (Albany NY). 2018; 10:1103–32. https://doi.org/10.18632/aging.101452 PMID:29779019

35. Olivieri F, Bonafè M, Spazzafumo L, Gobbi M, Prattichizzo F, Recchioni R, Marcheselli F, La Sala L, Galeazzi R, Rippo MR, Fulgenzi G, Angelini S, Lazzarini R, et al. Age- and glycemia-related miR-126-3p levels in plasma and endothelial cells. Aging (Albany NY). 2014; 6:771–87. https://doi.org/10.18632/aging.100693 PMID:25324472

36. Li Z, Zhou Y, Zhang L, Jia K, Wang S, Wang M, Li N, Yu Y, Cao X, Hou J. microRNA-199a-3p inhibits hepatic apoptosis and hepatocarcinogenesis by targeting PDCD4. Oncogenesis. 2020; 9:95. https://doi.org/10.1038/s41389-020-00282-y PMID:33099584

37. Chen HP, Wen J, Tan SR, Kang LM, Zhu GC. MiR-199a-3p inhibition facilitates cardiomyocyte differentiation of embryonic stem cell through promotion of MEF2C. J Cell Physiol. 2019; 234:23315–25. https://doi.org/10.1002/jcp.28899 PMID:31140610

38. Chung YP, Chen YW, Weng TI, Yang RS, Liu SH. Arsenic induces human chondrocyte senescence and accelerates rat articular cartilage aging. Arch Toxicol. 2020; 94:89–101. https://doi.org/10.1007/s00204-019-02607-2 PMID:31734849

39. Mazzucco AE, Smogorzewska A, Kang C, Luo J, Schlabach MR, Xu Q, Patel R, Elledge SJ. Genetic interrogation of replicative senescence uncovers a dual role for USP28 in coordinating the p53 and GATA4 branches of the senescence program. Genes Dev. 2017; 31:1933–38. https://doi.org/10.1101/gad.304857.117 PMID:29089421

40. Kang D, Shin J, Cho Y, Kim HS, Gu YR, Kim H, You KT, Chang MJ, Chang CB, Kang SB, Kim JS, Kim VN, Kim JH. Stress-activated miR-204 governs senescent phenotypes of chondrocytes to promote osteoarthritis development. Sci Transl Med. 2019; 11:eaar6659. https://doi.org/10.1126/scitranslmed.aar6659 PMID:30944169

41. Xia W, Zhu J, Wang X, Tang Y, Zhou P, Wei X, Chang B, Zheng X, Zhu W, Hou M, Li S. Overexpression of Foxc1 regenerates crushed rat facial nerves by promoting Schwann cells migration via the Wnt/β-catenin signaling pathway. J Cell Physiol. 2020; 235:9609–22. https://doi.org/10.1002/jcp.29772 PMID:32391604

42. Chang J, Wang Y, Shao L, Laberge RM, Demaria M, Campisi J, Janakiraman K, Sharpless NE, Ding S, Feng

W, Luo Y, Wang X, Aykin-Burns N, et al. Clearance of senescent cells by ABT263 rejuvenates aged hematopoietic stem cells in mice. Nat Med. 2016; 22:78–83.
https://doi.org/10.1038/nm.4010
PMID:26657143

43. Thompson PJ, Shah A, Ntranos V, Van Gool F, Atkinson M, Bhushan A. Targeted Elimination of Senescent Beta Cells Prevents Type 1 Diabetes. Cell Metab. 2019; 29:1045–60.e10.
https://doi.org/10.1016/j.cmet.2019.01.021
PMID:30799288

44. Crepin T, Carron C, Roubiou C, Gaugler B, Gaiffe E, Simula-Faivre D, Ferrand C, Tiberghien P, Chalopin JM, Moulin B, Frimat L, Rieu P, Saas P, et al. ATG-induced accelerated immune senescence: clinical implications in renal transplant recipients. Am J Transplant. 2015; 15:1028–38.
https://doi.org/10.1111/ajt.13092 PMID:25758660

45. Xie Z, Xia W, Hou M. Long intergenic non-coding RNA-p21 mediates cardiac senescence via the Wnt/β-catenin signaling pathway in doxorubicin-induced cardiotoxicity. Mol Med Rep. 2018; 17:2695–704.
https://doi.org/10.3892/mmr.2017.8169
PMID:29207090

46. Chen H, Xia W, Hou M. LncRNA-NEAT1 from the competing endogenous RNA network promotes cardioprotective efficacy of mesenchymal stem cell-derived exosomes induced by macrophage migration inhibitory factor via the miR-142-3p/FOXO1 signaling pathway. Stem Cell Res Ther. 2020; 11:31.
https://doi.org/10.1186/s13287-020-1556-7
PMID:31964409

47. Mathison M, Singh VP, Chiuchiolo MJ, Sanagasetti D, Mao Y, Patel VB, Yang J, Kaminsky SM, Crystal RG, Rosengart TK. *In situ* reprogramming to transdifferentiate fibroblasts into cardiomyocytes using adenoviral vectors: Implications for clinical myocardial regeneration. J Thorac Cardiovasc Surg. 2017; 153:329–39.e3.
https://doi.org/10.1016/j.jtcvs.2016.09.041
PMID:27773576

48. Zhuang L, Xia W, Chen D, Ye Y, Hu T, Li S, Hou M. Exosomal LncRNA-NEAT1 derived from MIF-treated mesenchymal stem cells protected against doxorubicin-induced cardiac senescence through sponging miR-221-3p. J Nanobiotechnology. 2020; 18:157.
https://doi.org/10.1186/s12951-020-00716-0
PMID:33129330

SUPPLEMENTARY MATERIAL

Supplementary Figure

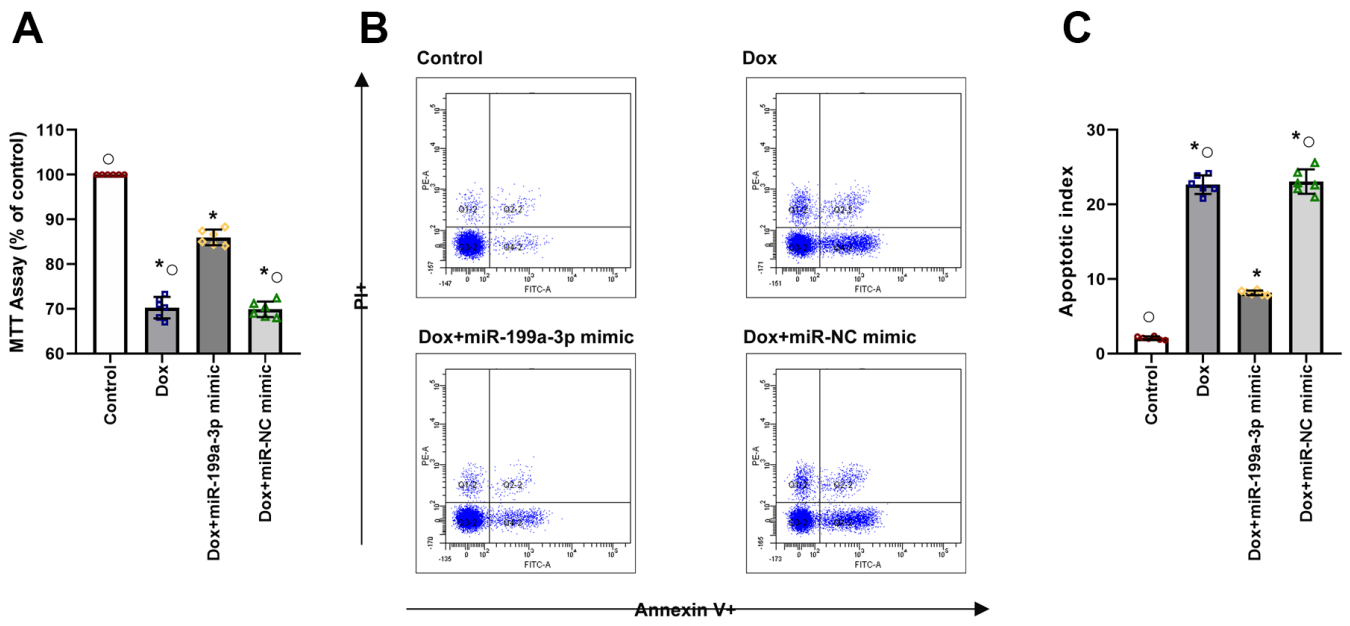

Supplementary Figure 1. Overexpression of miR-199a-3p took cellular protective effects against Dox. (**A**) Cell viability was analyzed with the MTT assay. (**B**, **C**) Representative flow cytometric dot plots of apoptotic cells after Annexin V/propidium iodide staining. $^{*}P < 0.05$ versus Control; $P < 0.05$ versus Dox +miR-199a-3p mimic in repeated-measures ANOVA, $n = 6$ per group.